Molecular Crystals and Liquid Crystals
Publication details, including instructions for authors and subscription information:
http://www.tandfonline.com/loi/gmcl20

Determination of the Landau's Coefficients for a Liquid Crystal Showing a De Vries Phase

Jean Marc Leblond [a b], Redouane Douali [a b], Yacine Cherfi [c], Nadir Beldjoudi [c], Adriana Wawrzyniak [d], Stanislaw Wróbel [d], Patrick Ropa [a b] & Christian Legrand [a b]

[a] Université Lille - Nord de France, Lille, France

[b] Université du Littoral Côte d'Opale, UDSMM, Calais, France

[c] Université de la Science et de la Technologie Houari Boumediene, Alger, Algérie

[d] Institut of Physics, Jagiellonian University, Reymonta, Krakow, Poland

Version of record first published: 30 Jun 2011

To cite this article: Jean Marc Leblond, Redouane Douali, Yacine Cherfi, Nadir Beldjoudi, Adriana Wawrzyniak, Stanislaw Wróbel, Patrick Ropa & Christian Legrand (2011): Determination of the Landau's Coefficients for a Liquid Crystal Showing a De Vries Phase, Molecular Crystals and Liquid Crystals, 541:1, 211/[449]-221/[459]

To link to this article: http://dx.doi.org/10.1080/15421406.2011.569234

Mol. Cryst. Liq. Cryst., Vol. 541: pp. 211/[449]–221/[459], 2011

ISSN: 1542-1406 print/1563-5287 online
DOI: 10.1080/15421406.2011.569234

Determination of the Landau's Coefficients for a Liquid Crystal Showing a De Vries Phase

JEAN MARC LEBLOND,[1,2] REDOUANE DOUALI,[1,2] YACINE CHERFI,[3] NADIR BELDJOUDI,[3] ADRIANA WAWRZYNIAK,[4] STANISLAW WRÖBEL,[4] PATRICK ROPA,[1,2] AND CHRISTIAN LEGRAND[1,2]

[1]Université Lille – Nord de France, Lille, France
[2]Université du Littoral Côte d'Opale, UDSMM, Calais, France
[3]Université de la Science et de la Technologie Houari Boumediene, Alger, Algérie
[4]Institut of Physics, Jagiellonian University, Reymonta, Krakow, Poland

A ferroelectric liquid crystal showing a de Vries phase is studied by the mean of dielectric and electro-optical measurements. Due to a strong electro-clinic effect close to the smectic A-smectic C* phase transition, a non linear electrical response is observed. The non linear dielectric characterization of this compound and the confrontation with a theoretical model allow us to extract the Landau's parameters of this material. The results are discussed on the basis of other data obtained by different measurement techniques. As an example, we confirm the second order smectic A*-smectic C* phase transition.*

Keywords de Vries phase; electro-clinic effect; Landau's parameters; non linear dielectric spectroscopy

1. Introduction

Several measurement techniques have been developed to characterize liquid crystals: Dielectric Spectroscopy, Electro-optical measurements, Differential Scanning Calorimetry, X-ray diffraction... [1,2]. For many years, Non Linear Dielectric Spectroscopy technique (NLDS) has paid attention for supplying information about various materials [4,5]. In liquid crystal materials, non linear effects can be observed within some phases and near the phase transitions [3]. The study of the non linear dielectric response coupled with a theoretical model can give access to some intrinsic parameters of many liquid crystals. For example, the use of this measurement technique in the SmC^* phase has already been used to determine some physical parameters: macroscopic polarization, viscosity and elastic energy [8]. In the case of SmA^* phase, the phenomenological model developed by Kimura links together the

Address correspondence to Jean Marc Leblond, Université Lille – Nord de France, F-59000 Lille, France. Tel.: 33(0)321994507; Fax: 33(0)321994501; E-mail: jean-marc.leblond@univ-littoral.fr

non linear dielectric response and the Landau's expansion development coefficients [9]. Due to a strong electro-clinic effect, the SmA* de Vries type phase does not require a high electric field to exhibit non linear effects. So, this phase should be a good candidate to compare experimental data with the theoretical model of Kimura. In this work, we have studied the FOOPP antiferro-electric liquid crystal to probe the non linear dielectric properties of the SmA* de Vries type phase.

2. Theortical Background

2.1. *Non Linear Dielectric Permittivities*

When a strong sinusoidal electric field $E(t)$ induces non linear effects in a dielectric material, we can see a distorted shape of the circulating current $I(t)$. A Fourier analysis can give the frequency harmonics of the spectra in terms of amplitude I_n and phase φ_n. Thus, the current $I(t)$ and the resulting electric displacement $D(t)$ can be written as follows:

$$I(t) = \sum_{n=1}^{n=\infty} I_n \cos(n\omega t + \varphi_n) \tag{1}$$

$$D(t) = \sum_{n=1}^{n=\infty} D_n \cos(n\omega t + \psi_n) \tag{2}$$

Using the complex notation I_n^* and D_n^* respectively complex amplitude of the $\boldsymbol{n}_{th}$ current and displacement harmonics are linked together taking account the area S of the sample:

$$D_n^* = \frac{I_n^*}{jn\omega S} \tag{3}$$

For the electric field $E(t)$ and the electric displacement $D(t)$ are no more in proportion, then $D(t)$ must be expressed into a power series of $E(t)$ with exponent $\boldsymbol{m}$:

$$D(t) = \sum_{m=1}^{m=\infty} [\alpha \cdot E\cos(\omega t)]^m \tag{4}$$

The non linear permittivities $\varepsilon_{\boldsymbol{n,m}}$ are finally defined when the terms of Eqs. (2) and (4) are identified by their same frequencies:

$$\begin{aligned} D_1^* &= \varepsilon_{1,1}^* E + \frac{3}{4}\varepsilon_{1,3}^* E^3 + \ldots\ldots\ldots \\ D_3^* &= \varepsilon_{3,3}^* E^3 + \frac{5}{16}\varepsilon_{3,5}^* E^5 + \ldots \\ D_5^* &= \varepsilon_{5,5}^* E^5 + \ldots\ldots\ldots \end{aligned} \tag{5}$$

From an experimental point of view, the main non linear permittivities $\boldsymbol{\varepsilon_{n,n}}$ are evaluated if the curves D_n^* versus E^n show a linear dependence. Only in these conditions, the $\mathbf{n}_{\text{th}}$-order non linear dielectric permittivity associates the $\mathbf{n}_{\text{th}}$-harmonic of the electric displacement D_n^* to the $\mathbf{n}_{\text{th}}$ power of the electric field E^n and the higher order inter-modulation

contribution terms $\varepsilon_{n,m}$ can be neglected. Let us notice that the first order non linear permittivity $\varepsilon_{1,1}$ is the same as the classical complex dielectric permittivity ε^* in the linear regime.

2.2. *Theoritical Model*

A phenomenological phase transition kinetic is described with the well known Landau's mean field model. The application of this model to the SmA*-SmC* phase transition gives the free energy density g. The tilt angle θ of the molecules in the smectic layers is the first order parameter and each FLC liquid crystal is identified in accordance with their own Landau's expansion coefficients as follows:

$$g = g_0 + \frac{\alpha}{2}(T - T_c)\theta^2 + \frac{b}{4}\theta^4 + \frac{P^2}{2\varepsilon_0\chi_0} - CP\theta - PE - \frac{1}{2}\varepsilon_0 E^2 \tag{6}$$

where g_0 represents the free energy density without electric field, T_c the SmA*- SmC* phase transition temperature, P the polarization, E the electric field, C the polarization-tilt coupling coefficient, α and b the Landau expansion coefficients, ε_0 and χ_0 the vacuum permittivity and the dielectric susceptibility.

By minimizing the free energy density from Eq. (6) respectively with θ and P, it leads to a set of equations traducing the electro-clinic effect as follows:

$$A\theta + B\theta^3 = E \tag{7}$$

where, $A = (T - T_c')/C\varepsilon_0\chi_0$, $B = b/C\varepsilon_0\chi_0$, $T_c' = T_c + C^2\varepsilon_0\chi_0/\alpha$. T_c' traduces the temperature shift of the phase transition because of the chiral contribution.

Referring to the above mentioned definitions of the non linear permittivities and assuming that the electric field is weak enough to neglect the higher order terms of Eq. (5), the theoretical expressions of $\varepsilon_{n,n}$ can be established on the basis of the following relations:

$$\varepsilon_{n,n} = \varepsilon_0\chi_0 C \lim_{\theta\to 0}\frac{\partial^n\theta}{\partial E^n} \tag{8}$$

This leads to the phenomenological model established by Kimura [9] traducing the non linear dielectric response by the mean of the first, third and fifth order non linear static permittivities.

$$\varepsilon^*_{1,1} = \varepsilon_0(1 + \chi_0) + \frac{C^2\varepsilon_0^2\chi_0^2}{\alpha(T - T_c')} \tag{9}$$

$$\varepsilon^*_{3,3} = -\frac{6bC^4\varepsilon_0^4\chi_0^4}{\alpha^4(T - T_c')^4} \tag{10}$$

$$\varepsilon^*_{5,5} = \frac{360b^2C^6\varepsilon_0^6\chi_0^6}{\alpha^7(T - T_c')^7} \tag{11}$$

3. Experimental Results

The measurement set-up depicted in Figure 1 has already been used to characterize non linear spectra of a ferroelectric liquid crystal in the SmC* phase [8]. A sine wave generator (Agilent 33210A) provides the applied sinusoidal electric field $E(t)$ across the cell measurement and the current $I(t)$ is obtained via a current amplifier (Keithley 428A). A voltage amplifier provides high level voltage if necessary. Both signals are digitalized and recorded with an acqusition board (PCI-DAS 4020/12) then displayed on a storage oscilloscope (HP 54600). The temperature is regulated with a heat stage Oxford IT 601. An HP VEE software has been developped to handle the complete set-up measurement and data collection in an automatic mode. The cell measurement has ITO electrodes of area $S = 23\,mm^2$ with rubbed PVA alignement layers. A gap provided by 13 µm spacers gives an empty cell capacity C_0 of 16 pF.

3.1. *Linear Dielectric Measurements*

First, a typical dielectric characterization has been performed in the linear regime and in a large temperature range. The classical soft mode has been studied in the SmA* and SmC* phases. As it can be seen in Figure 2, the frequency relaxation F_c and the inverse dielectric strength $\Delta\varepsilon^{-1}$ are linearly decreasing as predicted in the theory of the SmA* phase [11] with a sharp increase of $\Delta\varepsilon^{-1}$ on approching T_c'. The breaking of the slopes indicates the SmA*-SmC* phase transition at a measured temperature corresponding to $T_c' = 81,9°C$. This result is in accordance with the phase sequence given in Table 1.

3.2. *Non Linear Dielectric Measurements*

The $I(t)$ current's waveforms are reproduced in Figure 3 showing the influence of a growing electric field inside the SmA* domain. The temperature is stabilised at $T = 82{,}2°C$ and the frequency F of the applied sinusoidal voltage $V(t)$ is set to

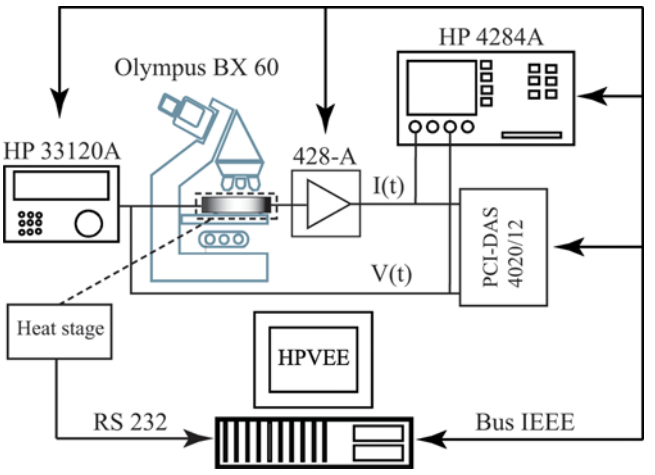

Figure 1. Experimental set-up used to measure the non linear dielectric response of the studied liquid crystal (FOOPP). (Figure appears in color online.)

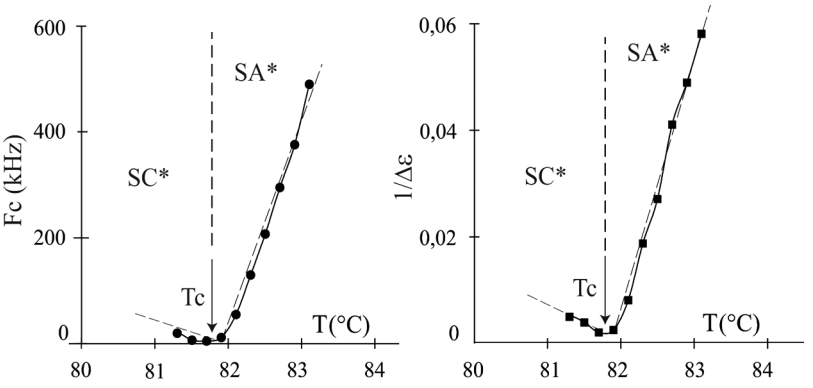

Figure 2. Variation of the frequency relaxation F_c and the opposite dielectric strength $\Delta\varepsilon^{-1}$ as a function of temperature in the vicinity of the SmA*-SmC* phase transition in the linear regime.

Table 1. Phase sequence of the compound FOOPP. (Transition temperatures in °C)

	Cr.-SmI*	SmI*-SmX*	SmX*-SmC*	SmC*-SmA*	SmA*-I
Heating	64,3	69,3	73,3	**80,8**	87,2
Cooling	53,5	70,0	73,6	**82,1**	87,7

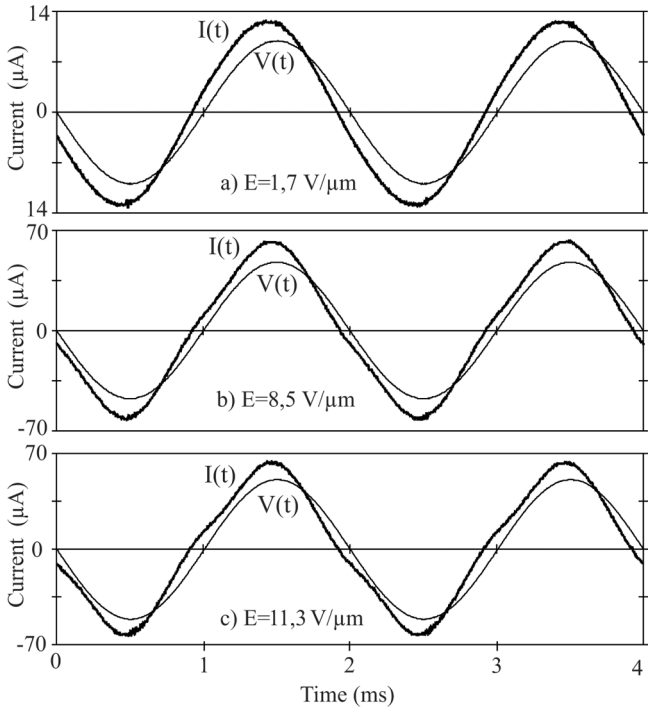

Figure 3. I(t) current and E(t) electric field waveforms measured at growing voltage levels. The suitable voltage level involves that D_3 and E^3 are in proportion.

$F = 500$ Hz. The non linear behaviour is clearly identified for $I(t)$ is no more sinusoidal. Note that the distortion of the current $I(t)$ in the SmA* phase requires a higher electric field (~ 8 V/μm) compared with the one used in the SmC* (~ 0.3 V/μm) [8]. Both signals $E(t)$ and $I(t)$ are nearly in phase which suggest a high conductivity effect.

In Figure 4, we give an example of a non linear dielectric spectrum $\varepsilon^*_{3,3}(F)$ obtained at a given temperature $T - T'_c = 1,9°C$. The conductivity effect is observed at low frequencies. We can see the relative constant value of the real part of $\varepsilon^*_{3,3}$ in a frequency range of 500 Hz–2 kHz. In order to reduce the influence of the conductivity, non linear static permittivities are measured at $F = 800$ Hz for each temperature. This frequency is consistent with the bandwidth of the set up measurement [8].

The first, third and fifth order non linear permittivities have been measured following the previous procedure. Nevertheless, the seventh order non linear permittivity could not have been evaluated with significant accuracy because of the set-up measurement's noise floor. The permittivities $\varepsilon^*_{1,1}$, $\varepsilon^*_{3,3}$ and $\varepsilon^*_{5,5}$ are not sufficient to determine the different parameters in Eqs. (9), (10) and (11). For this reason, non linear dielectric measurements have been completed by the characterization of the electro-clinic effect which can be described on the basis of the same theoretical model [12].

3.3. *Electro-Optical Measurements*

The experimental electro-optical measurements for the same compound FOOPP are depicted in Figure 5 and have been performed by A. Mikulko [12]. We can see the induced tilt angle θ plotted versus the applied electric field E for two temperatures in the SmA* phase ($T_1 = 83{,}1°C$ and $T_2 = 86{,}1°C$). The shapes of these curves are rather consistent with the predicted trend of Eq. (7) and lead us to determine the two parameters A and B which are linked to α, b, C and χ_0. The transition temperature T'_c was evaluated using the texture observation by the mean of a polarizing microscope. In Figure 5, the best fit of the E(θ) plots is given for two different

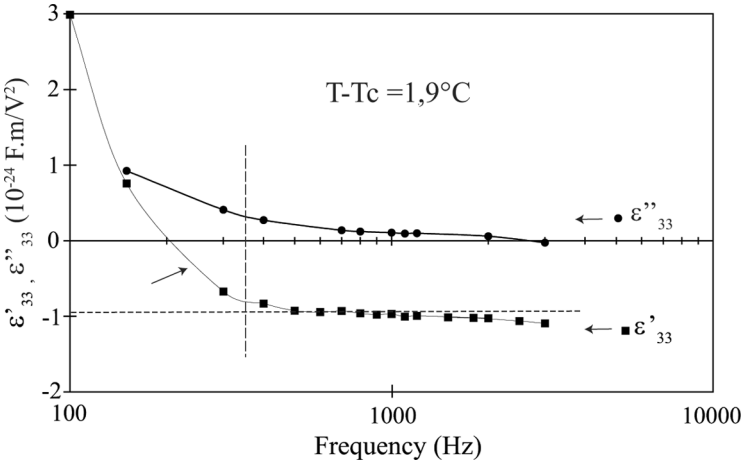

Figure 4. Third order non linear dielectric permittivity $\varepsilon^*_{3,3}$ in the low frequency domain. The straight line indicates the evaluated static value of the real part of $\varepsilon^*_{3,3}$.

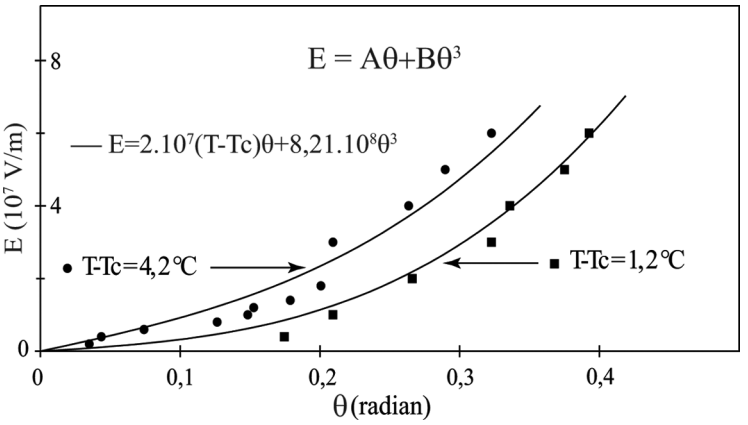

Figure 5. Electro-optical measurements for two reduced temperatures $(T - T_c')$. The straight lines indicate the best fitted curves.

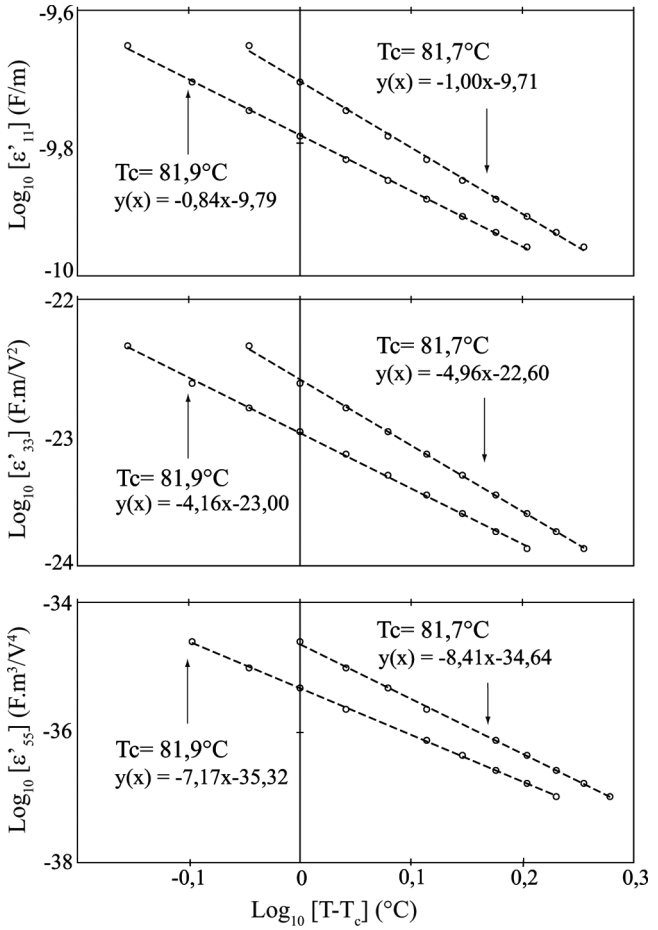

Figure 6. Temperature dependence of the static non linear permittivities $\varepsilon_{1,1}$, $\varepsilon_{3,3}$, $\varepsilon_{5,5}$ on a Log-Log scale. The solid lines represent the fit relative to Eq. (13).

temperatures in the vicinity of the phase transition: $E = 2.10^7(T - T'_c)\theta + 8,2.10^8\theta^3$. The main influence of the parameter B traduces the strong electro-clinic effect.

3.4. *Results Exploitation and Discussion*

As mentioned before, the Eqs. (9) to (11) show a temperature dependence of the static non linear permittivities. These equations can be transformed into a more suitable form expressed by the following power law where $\psi_{\text{theo.}}$ is the theoretical value of the denominator's exponent:

$$\varepsilon'_{n,n} = \frac{\rho_n}{(T - T'_c)^{\psi_{theo.}}} \tag{12}$$

The measured values of $\varepsilon'_{1,1}$, $\varepsilon'_{3,3}$ and $\varepsilon'_{5,5}$ versus temperature are shown in Figure 6 on a Log-Log scale and the value of T'_c previously determined ($T'_{c1} = 81,9°\text{C}$) was used to fit the data. In order to probe the influence of T'_c on the fitted data, another value of $T'_c(T'_{c2} = 81,7°\text{C})$ has been also used. The logarithmic scale shows a linear trend which is in accordance with Eq. (12).

Table 2. Comparison between theoretical and experimental values of the $(\text{T} - \text{T}'_\text{c})$ exponent term for two different temperature values near the SmA*-SmC* phase transition

Non linear permittivity	$\psi_{theo.}{}^a$	$\psi_{mes.}{}^b$ @ $\text{T}'_\text{c} = 81,7°\text{C}$	$\psi_{mes.}{}^b$ @ $\text{T}'_\text{c} = 81,9°\text{C}$
$\varepsilon'_{1,1}$	*1*	**1**	0,84
$\varepsilon'_{3,3}$	4	4,96	**4,16**
$\varepsilon'_{5,5}$	7	8,41	**7,17**

[a]The term $\psi^a_{theo.}$ is used in Eq. (13).
[b]Theo. and mes. denote respectively theoretical and experimental values.

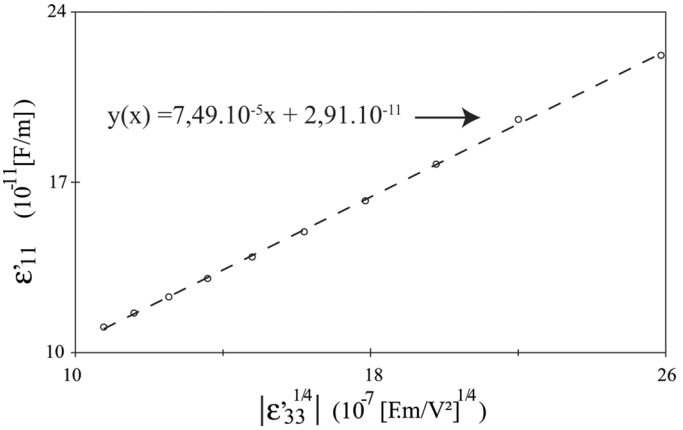

Figure 7. Evolution of $\varepsilon^*_{1,1}$ versus $|\varepsilon^*_{3,3}|^{1/4}$.

Table 3. Intermediate theoretical expressions, measurement techniques and corresponding numerical values

Theoretical Expressions	$\alpha/\varepsilon_0(1+\chi_0)$	$b/\varepsilon_0(1+\chi_0)$	$C^4[\varepsilon_0(1+\chi_0)]^4/6b$	$-6bC^4[\varepsilon_0(1+\chi_0)]^4/\alpha^4$
Technique of measurement	Electro-optical	Electro-optical	Non Lin. Diel. Spectroscopy	Non Lin. Diel. Spectroscopy
Numerical values	$2 \cdot 10^7$	$8{,}21 \cdot 10^8$	$3{,}14 \cdot 10^{-17}$	$-1{,}01 \cdot 10^{-23}$

Table 4. Landau expansion coefficients obtained for FOOPP liquid crystal

Coefficients	α ($Nm^{-2}\ rad^{-2}\ K^{-1}$)	b ($Nm^{-2}\ rad^{-4}$)	C (Vm^{-1})	χ_0
Numerical values	$0{,}65 \cdot 10^4$	$2{,}67 \cdot 10^5$	$0{,}16 \cdot 10^8$	2,29

The slopes of the logarithmic curves give access to the experimental exponent $\Psi_{mes.}$ and the best fit parameters are resumed in Table 2. Let us notice that for the experimental transition temperature $T'_{c1} = 81,9°C$, the gap between $\Psi_{mes.}$ and $\Psi_{theo.}$ is more important with the first order parameter $\varepsilon'_{1,1}$ but seems to be in good agreement with the theoretical expressions for $\varepsilon'_{3,3}$ and $\varepsilon'_{5,5}$. On the other hand, the use of $T'_{c2} = 81,7°C$ corresponds with the theoretical expressions for $\varepsilon'_{1,1}$ but not for the other non linear permittivities. Another way to exploit the data consists in using the relationship linking $\varepsilon'_{1,1}$ and $\varepsilon'_{3,3}$. Equation (13) predicts a linear evolution between $\varepsilon'_{1,1}$ and $|\varepsilon'_{3,3}|^{1/4}$ which is in accordance with the experimental plot (Fig. 7).

$$\varepsilon'_{1,1} = \varepsilon_0(1+\chi_0) + \frac{\varepsilon_0\chi_0 C}{(6b)^{\frac{1}{4}}} \cdot |\varepsilon'_{3,3}|^{\frac{1}{4}} \tag{13}$$

The fit of the data in Figures 6 and 7 using Eqs. (7) and (13) gives access to the different constants (Table 3). In Table 4, the corresponding numerical values of the Landau's expansion coefficients are presented. The estimated values are of the same order with other data coming from different measurement techniques [14]. The negative sign of the second Landau's expansion coefficient ***b*** traduces a second order phase transition. This in accordance with DSC analysis already done on the same material [13].

4. Conclusion and Perspectives

A non linear dielectric spectroscopy has been carried out to determine the Landau coefficients of a ferroelectric liquid crystal showing a de Vries phase. Significant results have been found in connection with a theoretical model and with other values published in the literature. Further experiments will be performed with a new set up measurement including a lock-in amplifier in order to improve higher harmonics sensitivity selection. In doing this, a better harmonic analysis performance will probably be obtained. Only using a non linear dielectric spectroscopy, the recording of all non-linear permittivities till the seventh order with sufficient accuracy may contribute to obtain the Landau's parameters regardless other measurements techniques.

References

[1] Manna, U., Song, J. K., Panarin, Yu. P., Fukuda, A., & Vij, J. K. (2008). *Phys. Rev. E*, *77*, 04170.
[2] Douali, R., Leroy, G., Gest, J., Tabourier, P., & Nguyen, H. T. (2000). *Eur. Phys. J. Appl. Phys.*, *9*, 25.
[3] Orihara, H., Fajar, A., & Bourny, V. (2002). *Phys. Rev. E*, *65*, 040701.
[4] Nakada, O. (1960). *J. Phys. Soc. Jpn.*, *15*, 2280.
[5] Kimura, Y., Hayakawa, R., & Okabe, N. (1997). *Mol. Cryst. Liq. Cryst.*, *304*, 275.

[6] Furukawa, T., Kodama, H., & Takahashi, Y. (1999). *Jpn. J. Appl. Phys.*, *38*, 3589.
[7] Garoff, S., & Meyer, R. B. (1977). *Phys. Rev. Lett.*, *38*, 848.
[8] Giesselman, F., Zuggenmaier, P., Dierking, I., Lagerwall, S. T., Stebler, B., Kaspar, M., Hamplova, V., & Glogarova, M. (1999). *Phys. Rev. E*, *60*, 598.
[9] Kimura, Y., Sako, T., & Hayakawa, R. (1993). *Ferroelectrics*, *14*, 315.
[10] Leblond, J. M., Douali, R., & Legrand, C. (2006). *Eur. Phys. J. Appl. Phys.*, *36*, 15.
[11] Blinc, R., & Zeks, B. (1978). *Phys. Rev. A*, *18*, 740.
[12] Mikulko, A., Marzec, M., Wrobel, S., Przedmojski, J., Douali, R., Legrand, C., Dabrowski, R., & Haase, W. (2006). *Chem. Phys. Lett.*, *431*, 289.
[13] Mikulko, A., Marzec, M., Wierzejska, M., Wrobel, S., Douali, R., Legrand, C., Dabrowski, R., & Haase, W. (2006). *Phase Trans.*, *79*, 585.
[14] Archer, P., Dierking, I., Görtz, V., & Goodby, J. W. (2008). *Eur. Phys. J. E.*, *25*, 385.